

Helix equations

Hans Drevermann

April 23, 2007

1 Abstract

The representation of helices in cylindrical coordinates can be very useful for the graphical representation of helices and for other applications.

We will show the graphical representations of helices in cylindrical coordinates, i.e. the projections ϕ/ρ , ϕ/z and ρ/z .

We will give exact and approximate mathematical representations of helices in cartesian and cylindrical coordinates. This leads to a better understanding of the respective graphical representations.

2 Introduction

Charged particles move in a magnetic field along curved tracks. Assuming an ideal homogeneous field and neglecting multiple scattering the tracks are described by helices. Depending on their charge the particles run clockwise (in ATLAS negative charge) or anticlockwise (in ATLAS positive charge) along their helices.

In ATLAS, as in many other experiments, most particles, mainly the interesting ones, leave the magnetic field after being only slightly bent. Thus, tracks are just helix segments. Practically all tracks of interest from one interaction in high energy physics stem from the same primary vertex or have an origin close to it.

3 Circle equations in cartesian coordinates

We define the z-axis of a cartesian coordinate system to run along the beam line, i.e. parallel to the magnetic field lines. We assume that the primary vertex lies exactly on the z-axis, i.e. it has the coordinates $x = 0$, $y = 0$ and $z = z_v$.

Figure 1 shows the y/x projection of a helix which is a circle¹. The circle passes at a minimum distance D_0 from the center of the coordinate system at P_0 . A particle running along this circle starts in the direction ϕ_0 . Therefore we give also the circle a direction ϕ_0 . A circle with a direction can be anticlockwise as in figure 1 or clockwise.

We will first discuss a circle which starts exactly from the primary vertex, i.e $D_0 = 0$, so that the points P_d and P_0 fall together. For an anticlockwise turning circle the angle $\Delta\alpha$ increases and $\Delta\alpha > 0$. We call this a positive turning circle with sign $S = +1$. Attention: this represents in ATLAS the track of a negative charged particle. A negative turning circle with decreasing azimuthal angle and $\Delta\alpha < 0$ has $S = -1$. For a positive (anticlockwise) turning circle the direction of the vertex as seen from the center of the coordinate system

¹Figures are found in black and white at the end of the paper.

P_0 is $\phi_0 + \frac{\pi}{2}$. For a negative (clockwise) turning circle the direction of the vertex is $\phi_0 - \frac{\pi}{2}$. R is the radius of the circle. The center point P_c of the circle has the coordinates x_c and y_c (see figure 1). x_c and y_c are given by:

$$x_c = R \cdot \cos(\phi_0 + S \cdot \frac{\pi}{2}) \quad y_c = R \cdot \sin(\phi_0 + S \cdot \frac{\pi}{2}) \quad (1)$$

$$x_c = -S \cdot R \cdot \sin \phi_0 \quad y_c = S \cdot R \cdot \cos \phi_0 \quad (2)$$

With $R_0 = S \cdot R$ one gets:

$$x_c = -R_0 \cdot \sin \phi_0 \quad y_c = R_0 \cdot \cos \phi_0 \quad (3)$$

If the circle does not pass through P_0 but in a distance of nearest approach D_0 (see figure 1) equation 3 changes to:

$$x_c = -(R_0 + D_0) \cdot \sin \phi_0 \quad y_c = (R_0 + D_0) \cdot \cos \phi_0 \quad (4)$$

This can be directly deduced from figure 1. If R_0 and D_0 have the same sign P_0 lies outside of the circle, otherwise inside. The coordinates x_d and y_d of the point of nearest approach P_d are given by:

$$x_d = -D_0 \cdot \sin \phi_0 \quad y_d = +D_0 \cdot \cos \phi_0 \quad (5)$$

The coordinates x, y of points on the circle with an angle $\Delta\alpha$ as seen from P_c are given by:

$$x = x_c + R_0 \cdot \sin(\phi_0 + \Delta\alpha) \quad y = y_c - R_0 \cdot \cos(\phi_0 + \Delta\alpha) \quad (6)$$

As a test, one gets from equation 4 for $\Delta\alpha = 0$ the coordinates of P_d given by equation 5. To draw a circle segment of $\frac{\pi}{2}$ from P_d for positive turning circles $\Delta\alpha$ varies from 0 to $+\frac{\pi}{2}$, for negative turning circles from 0 to $-\frac{\pi}{2}$. R_0 and $\Delta\alpha$ have always the same sign.

In HEP experiments one may find tracks of very high momentum, so that R_0 approaches infinity. Measuring errors of the space points, from wheach the track was reconstructed, may increase R_0 furthermore. In this case the use of the equations 6 may lead to errors, as one has to deal with small values being the differenc of very large ones. This is avoided, if one calculates points on the helix by use of equations in polar coordinates.

3.1 Helix equation in carthesian coordinates

Giving the points of the circle a third coordinate z one gets a helix. z is defined by:

$$z = z_0 + \tan \lambda_0 \cdot R_0 \cdot \Delta\alpha \quad z - z_0 = \Delta z \quad (7)$$

where z_0 is the z coordinate of P_d and λ_0 the angle between a tangential line of the helix and the xy-plane ($\tan \lambda_0 = \frac{P_Z}{P_T}$, $P_T = \sqrt{P_X^2 + P_Y^2}$). As R_0 and $\Delta\alpha$ have always the same sign, Δz and $\tan \lambda_0$ have the same sign.

In a homogeneous solenoidal field R_0 is proportional to the strength and direction of the magnetic field B (negative in the case of ATLAS) and to the transverse momentum P_T of the particle.

$$R_0 = \frac{P_T}{s \cdot e \cdot B} \quad (8)$$

where e is the elementary charge and s the sign of the charge of the particle. Then one gets:

$$\tan \lambda_0 \cdot R_0 = \frac{P_Z}{P_T} \cdot R_0 = \frac{P_Z}{s \cdot e \cdot B} \quad (9)$$

Attention: P_d is not the point of nearest approach of the helix to the center of the coordinate system, i.e. in 3D, but the point of nearest approach of the circle to the z-axis, i.e. in the y/x projection, which means in 2D. This 2D point becomes a 3D point with z_0 as z-coordinate.

A helix, which has at the point of nearest approach P_d the coordinates x_d, y_d (see equation 4 and z_0 is defined by the parameters $R_0, D_0, \phi_0, \tan \lambda_0$ and z_0 . They are called perigee parameters. Instead of R_0 sometimes $\frac{1}{R_0}$ or s^*P_T are used. Attention: there may be different definitions of the signs of R_0 and D_0 . Instead of $\tan \lambda_0$ one may use a function of $\tan \lambda_0$ as e.g. η . This must be taken into account, when applying these equations. The perigee parameters describe a helix, but not a helix segment with end points.

In HEP experiments one may find tracks of very high momentum, so that R_0 approaches infinity. Measuring errors of the space points, from which the track was reconstructed, may increase R_0 furthermore. In this case the use of the equations 6 may lead to errors, as one has to deal with small values being the difference of very large ones. This is avoided, if one calculates points on the helix by use of equations in polar coordinates.

4 Helix equations in cylindrical coordinates

A point P on the circle has the polar coordinates $\Delta\phi'$ and ρ' as seen from P_d and $\Delta\phi$ and ρ as seen from P_0 (see ed_h2.pdf a):

$$\tan \phi = y/x \quad \rho^2 = x^2 + y^2 \quad (10)$$

The ϕ value of a point on the circle starting at P_d in a direction ϕ_0 is given by (see figure 2b):

$$\phi = \phi_0 + \Delta\phi \quad (11)$$

Figure 2b shows ϕ as a function of ρ in red, if $D_0 = 0$, and in white, if $D_0 \neq 0$. The white line superimposes the red one for larger ρ values. The green line is the linear extrapolation of the red one, in order to illustrate the non linear behaviour of the white and the red curves for larger ρ values.

ρ and ϕ together with the third coordinate z as defined in equation 7 define the cylindrical coordinates of points along the helix.

To show a function $v=v(h)$ graphically, a graph of v on the vertical axis versus h on the horizontal axis is normally presented. If one shows points, whose position is described by the function, one speaks of a v/h projection of the points and in the same way one can speak of a v/h projection of the function.

It is of interest to understand ϕ as a function of ρ : $\phi(\rho)$, as well as ϕ as a function of z : $\phi(z)$, and ρ as a function of z : $\rho(z)$.

Figure 3 shows a helix in 3 projections: ϕ/ρ (figure 3a), ϕ/z (figure 3b) and ρ/z (figure 3c). The respective magnified projections are shown in the figure 3d to figure 3f.

Three regions are clearly visible:

- the inner region, where
 - ϕ/ρ and ϕ/z deviate strongly (by 90°) from linearity,
 - ρ/z deviates very slightly from linearity;
- the middle region, where the functions are linear;
- the outer region, where
 - ϕ/ρ and ρ/z deviate from linearity,
 - ϕ/z remains linear.

In the following the equations for $\phi(\rho)$, $\phi(z)$ and $\rho(z)$ will be given

- exactly: covering the three regions
- approximately: for each region separatly.

4.1 Exact helix equations in cylindrical coordinates

A positive turning circle is shown in figure 2a. From the figure one can derive 3 basic equations:

$$\Delta\phi' = \frac{\Delta\alpha}{2} \tag{12}$$

$$\frac{\rho'}{2R_0} = \sin(\Delta\phi') \quad (13)$$

With equation 7 ($\Delta z = \tan \lambda_0 \cdot R_0 \cdot \Delta\alpha$) one gets:

$$\Delta z = \tan \lambda_0 \cdot R_0 \cdot 2\Delta\phi' \quad (14)$$

In the case of a positive turning circle R_0 and $\Delta\phi'$ are both positive, in the case of a negative turning circle R_0 and $\Delta\phi'$ are both negative, so that the sign of Δz depends only on $\tan \lambda_0$, as it should.

If $D_0 = 0$ i.e. $\Delta\phi' = \Delta\phi$ and $\rho' = \rho$ one gets:

$$\Delta\phi = \frac{\Delta\alpha}{2} \quad (15)$$

For $\phi(\phi/\rho)$ one gets:

$$\sin(\Delta\phi) = \frac{\rho}{2R_0} \quad (16)$$

For $\phi(z)$ one gets:

$$\Delta\phi = \frac{\Delta z}{2R_0 \cdot \tan \lambda_0} \quad (17)$$

From the equations 16 and 17 one gets for $\rho(z)$:

$$\rho = 2R_0 \cdot \sin \frac{\Delta z}{2R_0 \cdot \tan \lambda_0} \quad (18)$$

The equations 16 to 18 give the exact description of a helix in polar coordinates if $D_0 = 0$.

If $D_0 \neq 0$ they are much more complicated: The equations for $\phi(\rho)$ are calculated in appendix 1. With

$$R_1 = R_0 + D_0 \quad D_1 = D_0 \cdot \left(1 - \frac{D_0}{2R_1}\right) \quad (19)$$

one gets:

$$\sin(\phi - \phi_0) = \sin \Delta\phi = \frac{D_1}{\rho} + \frac{\rho}{2R_1} \quad (20)$$

The respective equations for $\phi(z)$ and $\rho(z)$ are calculated in appendix 2 and 3:

$$\tan(\phi - \phi_0) = \tan \Delta\phi = \frac{D_0}{R_0 \cdot \sin \frac{\Delta z}{R_0 \cdot \tan \lambda_0}} + \tan \frac{\Delta z}{2R_0 \cdot \tan \lambda_0} \quad (21)$$

$$\rho^2 = D_0^2 + \left(1 + \frac{D_0}{R_0}\right) \cdot 4R_0^2 \cdot \sin^2 \frac{\Delta z}{2R_0 \cdot \tan \lambda_0} \quad (22)$$

If $D_0 = 0$, the equations 20 and 21 give back the equations 16 and 17.

4.2 Approximation in the inner and linear regions.

We assume $D_0 \ll R_0$ and $\frac{\Delta z}{\tan \lambda_0} \ll R_0$.

For $\phi(\rho)$ (equation 20) one gets::

$$\sin \Delta\phi \approx \frac{D_0}{\rho} + \frac{\rho}{2R_0} \quad (23)$$

For $\phi(z)$ (equation 21) one gets::

$$\tan \Delta\phi \approx \frac{D_0 \cdot \tan \lambda_0}{\Delta z} + \frac{\Delta z}{2R_0 \cdot \tan \lambda_0} \quad (24)$$

For $\rho(z)$ (equation 22) one gets::

$$\rho^2 \approx D_0^2 + \left(\frac{\Delta z}{\tan \lambda_0} \right)^2 \quad (25)$$

The border between the inner region and the linear region lies at the position, where the 2 terms of the addition in the 3 equations above are equal:

For $\phi(\phi/\rho)$ (equation 23) one gets:

$$\rho_{\phi/\rho} = \sqrt{2R_0 \cdot D_0} \quad (26)$$

For $\phi(z)$ (equation 24) one gets:

$$\Delta z_{\phi/z} = \tan \lambda_0 \cdot \sqrt{2R_0 \cdot D_0} \quad (27)$$

For $\rho(z)$ (equation 25) one gets for $\rho(z)$:

$$\Delta z_{\rho/z} = D_0 \cdot \tan \lambda_0 \quad (28)$$

Depending on the value of ρ or Δz the left or the right term of the respective sum in the equations 23 to 25 is dominant.

The border between the 2 regions is practically the same for $\phi(\rho)$ and $\phi(z)$, but much closer to 0 for $\rho(z)$.

4.3 Approximation in the inner region

For $\phi(\rho)$ one gets:

$$\sin \Delta\phi \approx \frac{D_0}{\rho} \quad (29)$$

For $\phi(z)$ one gets:

$$\tan \Delta\phi \approx \frac{D_0 \cdot \tan \lambda_0}{\Delta z} \quad (30)$$

For $\rho(z)$ one gets:

$$\rho \approx |D_0| \quad (31)$$

With $\frac{\Delta z}{\tan \lambda_0} \approx \rho'$ (see equations 13 and 14) one can change the equations 25 and 30 to:

$$\tan \Delta\phi \approx \frac{D_0}{\rho'} \quad (32)$$

$$\rho^2 \approx D_0^2 + \rho'^2 \quad (33)$$

The equations 29, 32 and 33 follow directly from figure 2c which replaces figure 2a in the case $R_0 = \infty$.

4.4 Approximation in the linear region

Most HEP detectors are built in a way, that the space points of tracks of interesting particles lie on helix segments, which are only slightly curved up to the last measured space point. The distance of the first measured space point to the beam line is significantly bigger than the D_0 of interesting tracks. Helix segments lie in the linear range as long as

$$\frac{D_0}{\rho} < E_\phi \quad , \quad \frac{D_0 \cdot \tan \lambda_0}{\Delta z} < E_\phi \quad , \quad (34)$$

$$|\Delta\phi - \sin \Delta\phi| < E_\phi \quad \text{and} \quad |\Delta\phi - \tan \Delta\phi| < E_\phi \quad (35)$$

where E_ϕ is the measuring error of ϕ (see equations 23 and 24). For $\rho(z)$ the range extends to lower values of z , i.e. $\frac{\Delta z}{\tan \lambda_0} \gg D_0$.

For $\phi(\rho)$ one gets then:

$$\Delta\phi \approx \frac{\rho}{2R_0} \quad (36)$$

For $\phi(z)$ one gets:

$$\Delta\phi \approx \frac{\Delta z}{2R_0 \cdot \tan \lambda_0} \quad (37)$$

For $\rho(z)$ one gets:

$$\rho \approx \frac{\Delta z}{\tan \lambda_0} \quad (38)$$

By replacing R_0 and $\tan \lambda_0$ by P_T and P_Z (see equations 8 and 9) one gets:

$$\Delta\phi \approx s \cdot e \cdot B \cdot \frac{\rho}{2P_T} \quad (39)$$

$$\Delta\phi \approx s \cdot e \cdot B \cdot \frac{\Delta z}{2P_Z} \quad (40)$$

$$\frac{\Delta z}{\rho} \approx \frac{P_Z}{P_T} \quad (41)$$

4.5 Approximation in the linear and outer region

The approximation in the linear and outer region are identical to the exact equations 16 to 18, which were derived for the case $D_0 = 0$.

4.6 λ as a function of ρ

In the linear region of $\rho(z)$ the polar angle λ_0 is constant (see figure 3c and 3f).

$$\tan \lambda_0 = \frac{\Delta z}{\rho} = \frac{P_Z}{P_T} \quad (42)$$

Several tracks may have different values of z_0 , which may be due to measuring errors, to multiple scattering or to a secondary vertex from which the track originates. In pattern recognition the z-position z_v of the primary vertex is determined, which lies on the z-axis, i.e. $x_v = 0$ and $y_v = 0$. If the angle λ is seen from the primary vertex P_V , it is no longer constant close to the vertex (see figure 4).

$$\tan \lambda = \frac{z - z_v}{\rho} \quad (43)$$

From appendix 4 one gets:

$$\tan \lambda = \tan \lambda_0 + \frac{z_0 - z_v}{\rho} \quad (44)$$

The behaviour is similar to the one of $\phi(\rho)$ close to the vertex, compare to equation 29.

5 Linearisation of $\phi(\rho)$ for visual pattern recognition

In HEP experiments it is sometimes of interest to identify points which belong to the same helix, even in an environment of points belonging to other helices or of points due to noise. We assume here that we are outside of the inner region, i.e. D_0 and multiple scattering are sufficiently small.

If the radius of such a helix is sufficiently large the points should lie on a straight line in a ϕ/ρ , a ϕ/z or a ρ/z projection according to the equations 36, 37 and 38 and can be identified as such.

If the radius is not large enough, they lie on a straight line in a ϕ/z projection (see equation 17). However, if one cannot approximate $\sin \Delta\phi$ by $\Delta\phi$, they lie on a more or less curved line in the other projections (see equations 16 and 18). In the case of the ϕ/ρ projection there is a method of linearisation:

Setting in Equation 16 $\sin(\phi - \phi_0) = \sin \phi \cdot \cos \phi_0 - \cos \phi \cdot \sin \phi_0$ and dividing by $\cos \phi \cdot \cos \phi_0$ one gets for the case $D_0 = 0$:

$$\tan \phi \approx \frac{1}{2R_0 \cdot \cos \phi_0} \cdot \frac{\rho}{\cos \phi} + \tan \phi_0 \quad (45)$$

If one rotates the coordinate system by an arbitrary angle $-\phi_1$ one gets:

$$\tan(\phi - \phi_1) \approx \frac{1}{2R_0 \cdot \cos(\phi_0 - \phi_1)} \cdot \frac{\rho}{(\cos \phi - \phi_1)} + \tan(\phi_0 - \phi_1) \quad (46)$$

If one makes a projection of $\tan(\phi - \phi_1)$ versus $\frac{\rho}{\cos(\phi - \phi_1)}$ one gets again a straight line.

If one sets $\phi_1 \approx \phi_0$ or to the ϕ value of one of the points in question $\tan(\phi - \phi_1)$ is not very different from $\phi - \phi_1$ and $\frac{\rho}{\cos(\phi - \phi_1)}$ is not very different from ρ . Therefore, this projection looks similar to the ϕ/ρ projection, except that the points of the helix lie now on a straight line.

6 Determination of the perigee parameters

From the cylindrical coordinates of 2 points on a circle one can calculate the perigee parameters from equations 36 or 37 and 38, if the points lie in the linear region. In that case D_0 cannot be calculated and is set to 0. R_0 , ϕ_0 and z_0 are found by solving a set of linear equations.

If the points lie in the linear and the outer region R_0 and ϕ_0 can be calculated by solving linear equations, via equation 45 and D_0 is set to 0.

If one wants to calculate D_0 as well, one needs 3 points of which at least one should be sufficiently close to the inner region, so that its offset from a straight line is larger than the measuring errors.

In order to calculate R_0 , ϕ_0 and D_0 by use of linear equations, one needs to modify equation 20 in the same way equation 45 was deduced.

Setting in Equation 20 $\sin(\phi - \phi_0) = \sin \phi \cdot \cos \phi_0 - \cos \phi \cdot \sin \phi_0$ and dividing by $\cos \phi \cdot \cos \phi_0$ one gets:

$$\tan \phi = \tan \phi_0 + \frac{D_1}{\cos \phi_0} \cdot \frac{1}{\rho \cdot \cos \phi} + \frac{1}{2R_1 \cdot \cos \phi_0} \cdot \frac{\rho}{\cos \phi} \quad (47)$$

Solving this equation for 3 points one gets $\tan \phi_0$, $\frac{D_1}{\cos \phi_0}$ and $\frac{1}{2R_1 \cdot \cos \phi_0}$ from which one can calculate R_0 and ϕ_0 and D_0 .

To calculate $\tan \lambda_0$ and z_0 one can use equation 38, with a linear region reaching far down to 0. Two points are sufficient, which, however, must not lie in the outer region.

7 Conclusions

The calculation of space points along a circle or helix close to the point of nearest approach may lead to numerical problems if the radius R_0 is very large and one uses the simple cartesian equations 6, because one calculates small numbers by subtracting very large ones. This problem is avoided if one calculates the cylindrical space points via equations 19 to 22.

As already stated in section 4.4, most HEP detectors are built in a way, that the space points of tracks of interesting particles lie on helix segments, which are only slightly curved up to the last measured space point. As the distance of the first measured space point to the beam line is normally significantly bigger than the D_0 of interesting tracks, the measured space points lie in the linear range of $\phi(\rho)$, $\phi(z)$ and $\rho(z)$. These functions are described by the very simple set of linear equations 36 to 41.

The linear behaviour of these function leads to helix projections ϕ/ρ , ϕ/z , ρ/z and ϕ/λ , which ease considerably detection and analysis of particle tracks through their measured space points.

The deviations from linearity are due to the approximation of $\sin \Delta\phi$ by $\Delta\phi$ and a behaviour of $\phi(\rho)$ and $\phi(z)$ very close to the vertex described by $\frac{1}{\rho}$ and $\frac{1}{\Delta z}$ respectively.

8 Appendix 1: $\phi(\rho)$

From figure 2a one gets:

$$U = \rho \cdot \cos \Delta\phi \quad V = \rho \cdot \sin \Delta\phi \quad (48)$$

$$U = R_0 \cdot \sin \Delta\alpha \quad V = R_0 + D_0 - \rho \cdot \cos \Delta\alpha \quad (49)$$

$$\rho \cdot \cos \Delta\phi = R_0 \cdot \sin \Delta\alpha \quad R_0 + D_0 - \rho \cdot \sin \Delta\phi = R_0 \cdot \cos \Delta\alpha \quad (50)$$

with

$$R_1 = R_0 + D_0 \quad (51)$$

one gets by squaring and adding the equations 50:

$$R_1^2 - 2R_1 \cdot \rho \cdot \sin \Delta\phi + \rho^2 \cdot \sin^2 \Delta\phi + \rho^2 \cdot \cos^2 \Delta\phi = R_0^2 \quad (52)$$

$$R_1^2 - R_0^2 + \rho^2 = 2R_1 \cdot \rho \cdot \sin \Delta\phi \quad (53)$$

$$\frac{R_1^2 - R_0^2}{2R_1 \cdot \rho} + \frac{\rho^2}{2R_1 \cdot \rho} = \sin \Delta\phi \quad (54)$$

With

$$D_1 = \frac{R_1^2 - R_0^2}{2R_1} = \frac{R_1^2 - R_0^2 + 2R_1 \cdot D_0 - D_0^2}{2R_1} \quad (55)$$

$$D_1 = D_0 \cdot \left(1 - \frac{D_0}{2R_1}\right) \quad (56)$$

one gets the final result:

$$\frac{D_1}{\rho} + \frac{\rho}{2R_1} = \sin \Delta\phi \quad (57)$$

9 Appendix 2: $\phi(z)$

Equations 14 and 13 are used below:

$$\frac{\Delta z}{\tan \lambda_0} = 2R_0 \cdot \Delta\phi' \quad \frac{\rho'}{2R_0} = \sin \Delta\phi' \quad (58)$$

From figure 2a one gets:

$$U = \rho' \cdot \cos \Delta\phi' \quad V = D_0 + \rho' \cdot \sin \Delta\phi' \quad (59)$$

$$\tan \Delta\phi = \frac{V}{U} = \frac{D_0 + \rho' \cdot \sin \Delta\phi'}{\rho' \cdot \cos \Delta\phi'} \quad (60)$$

Replacing ρ' via equation 58 (right) one gets:

$$\tan \Delta\phi = \frac{D_0}{2R_0 \cdot \sin \Delta\phi' \cdot \cos \Delta\phi'} + \tan \Delta\phi' \quad (61)$$

$$\tan \Delta\phi = \frac{D_0}{R_0 \cdot \sin 2\Delta\phi'} + \tan \Delta\phi' \quad (62)$$

This equation gives $\Delta\phi$ as function of $\Delta\phi'$. Replacing $\Delta\phi'$ via equation 58(left) one gets the final result:

$$\tan \Delta\phi = \frac{D_0}{R_0 \cdot \sin \frac{\Delta z}{R_0 \cdot \tan \lambda_0}} + \tan \frac{\Delta z}{2R_0 \cdot \tan \lambda_0} \quad (63)$$

10 Appendix 3: $\rho(z)$

Equations 14 and 13 are used below (as equations 58):

$$\frac{\Delta z}{\tan \lambda_0} = 2R_0 \cdot \Delta\phi' \quad \frac{\rho'}{2R_0} = \sin \Delta\phi' \quad (64)$$

From figure 2a one gets(as equations 59):

$$U = \rho' \cdot \cos \Delta\phi' \quad V = D_0 + \rho' \cdot \sin \Delta\phi' \quad (65)$$

$$\rho^2 = U^2 + V^2 = \rho'^2 + D_0^2 + 2D_0 \cdot \rho' \cdot \sin \Delta\phi' \quad (66)$$

Replacing $\sin \Delta\phi'$ via equation 64 (right) one gets:

$$\rho^2 = D_0^2 + \rho'^2 + \frac{2D_0 \cdot \rho'^2}{2R_0} \quad (67)$$

$$\rho^2 = D_0^2 + \rho'^2 \cdot \left(1 + \frac{D_0}{R_0}\right) \quad (68)$$

Replacing ρ' via the equations 64 one gets the final result:

$$\rho^2 = D_0^2 + \left(1 + \frac{D_0}{R_0}\right) \cdot 4R_0^2 \cdot \sin^2 \cdot \frac{\Delta z}{2R_0 \cdot \tan \lambda_0} \quad (69)$$

11 Appendix 4: $\lambda(\rho)$

From figure 4 one gets:

$$\frac{z - z_0}{\rho} = \tan \lambda_0 \quad \frac{z - z_v}{\rho} = \tan \lambda \quad (70)$$

From this follows the final result:

$$\tan \lambda = \tan \lambda_0 + \frac{z_0 - z_v}{\rho} \quad (71)$$


```

c ----- <<<<< >>>>>>>>>
c ..... all angles in radians.  if r0<0 then dalpha<0 !
c if(r0*dalpha.lt.0.) then
c   terr='r0*dalpha.lt.0.'
c else
c   terr=' '
c ..... equations 6,7
c   x=xc+r0*sin(fi0+dalpha)
c   y=yc-r0*cos(fi0+dalpha)
c   z=z0+tan(alambda0)*r0*dalpha
c   terr=' '
c end if
c return

c entry get_point_at_rho(rho,x,y,z,terr)
c ----- <<< >>>>>>>>>
c if(rho.lt.d0) then
c   terr='rho.lt.d0'
c else
c   terr=' '
c ..... equation 20
c   if(rho.eq.d0) then
c     sindf=1.
c   else
c     ..... If(rho=d0), sindf may be numeriacally just bigger 1.
c     sindf=d1/rho+rho/(2.*r1)
c   end if
c   df=asin(sindf)
c   x=rho*cos(fi0+df)
c   y=rho*sin(fi0+df)
c ..... equation 22 inversed
c   sq=sqrt((rho*rho-d0*d0)/(1.+d0/r0))
c   as=asin(sq/(2.*r0))
c   dz=2.*rtl*as
c   z=z0+dz

c end if
c return

c entry get_point_at_rhoprime(rhop,x,y,z,terr)
c ----- <<<< >>>>>>>>>
c if(rhop.lt.0) then
c   terr='rhop.le.0'

```



```

else
  terr=' '
c ..... equation 16
  sindf=rhop/(2.*r0)
  df=asin(sindf)
  xp=rhop*cos(fi0+df)
  yp=rhop*sin(fi0+df)
  x=xd+xp
  y=yd+yp
c ..... equation 18 inversed
  as=asin(rho/(2.*r0))
  dz=2.*rtl*as
  z=z0+dz

end if
end

```

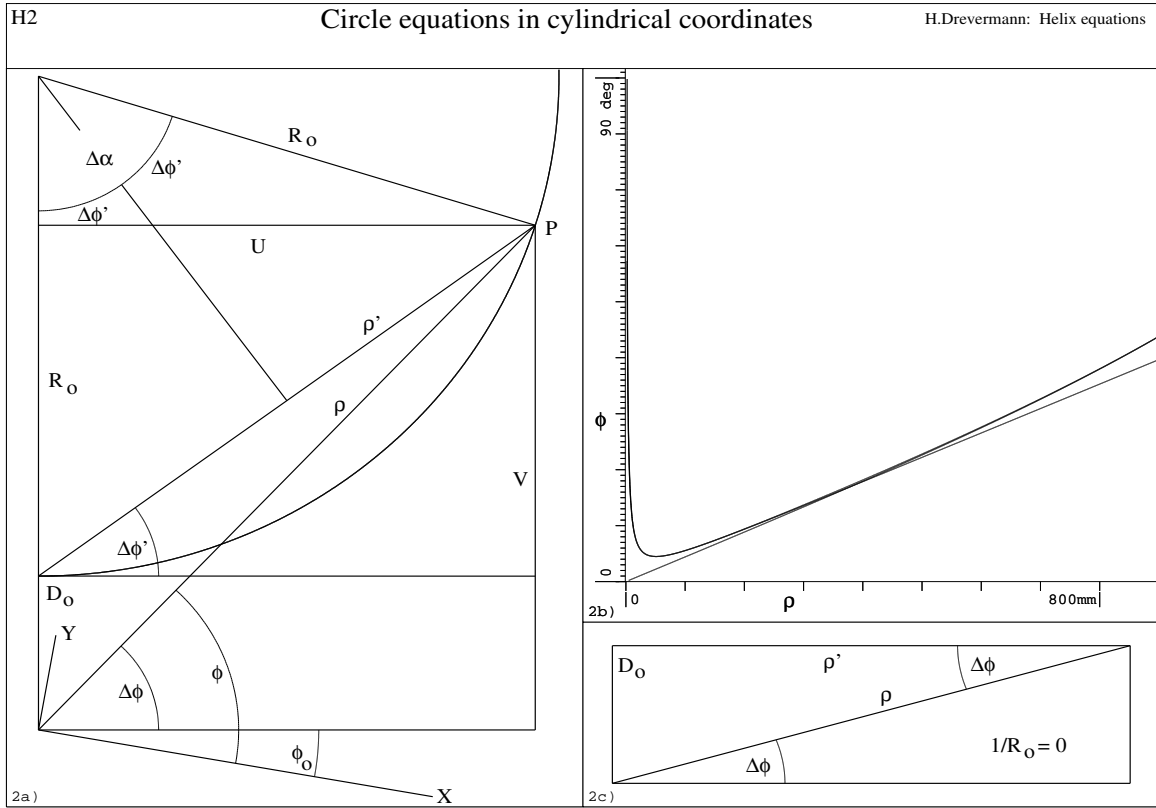



Figure 2: "Circle equations in cartesian coordinates"

The pdf file ed_bw_h2.pdf contains the figure in black and white.

The pdf file ed_co_h2.pdf contains the figure in color. When displaying the color picture the quality is better, if acroread is used.

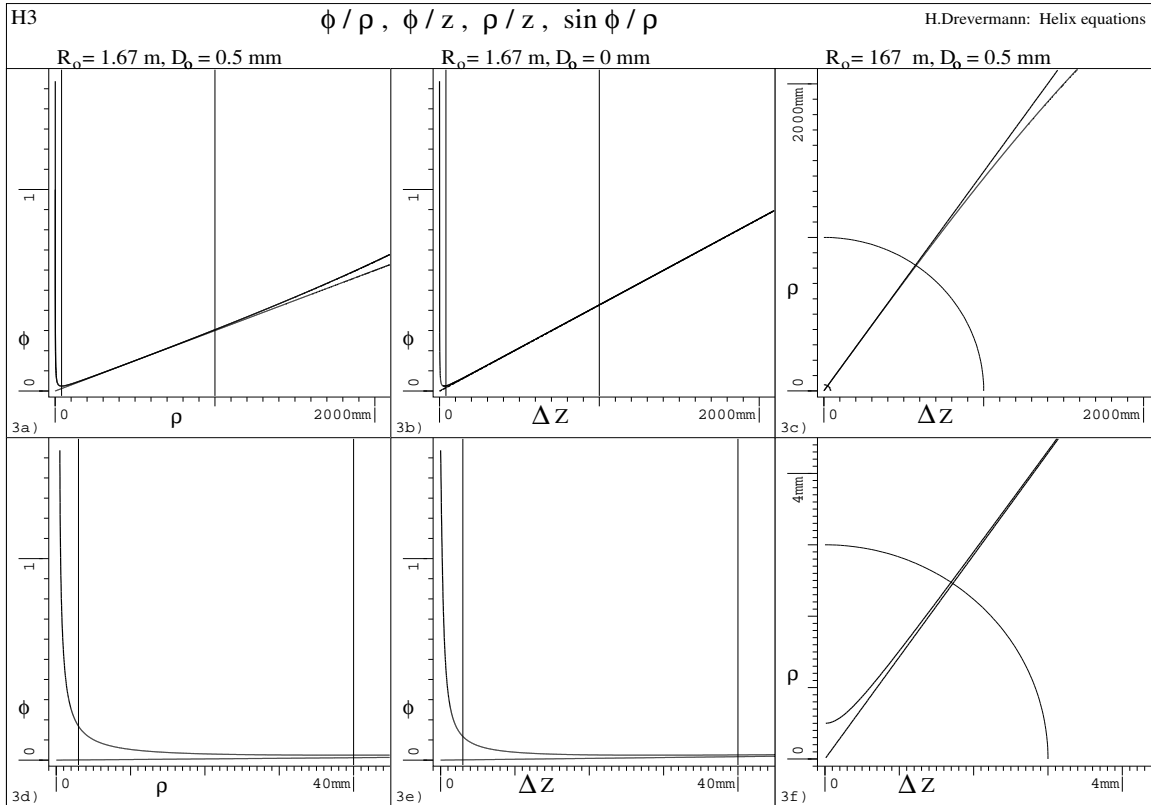


Figure 3: " $\phi/\rho, \phi/z$ and ρ/z projection of aa helix"

The pdf file ed_bw_h3.pdf contains the figure in black and white.

The pdf file ed_co_h3.pdf contains the figure in color. When displaying the color picture the quality is better, if acroread is used.

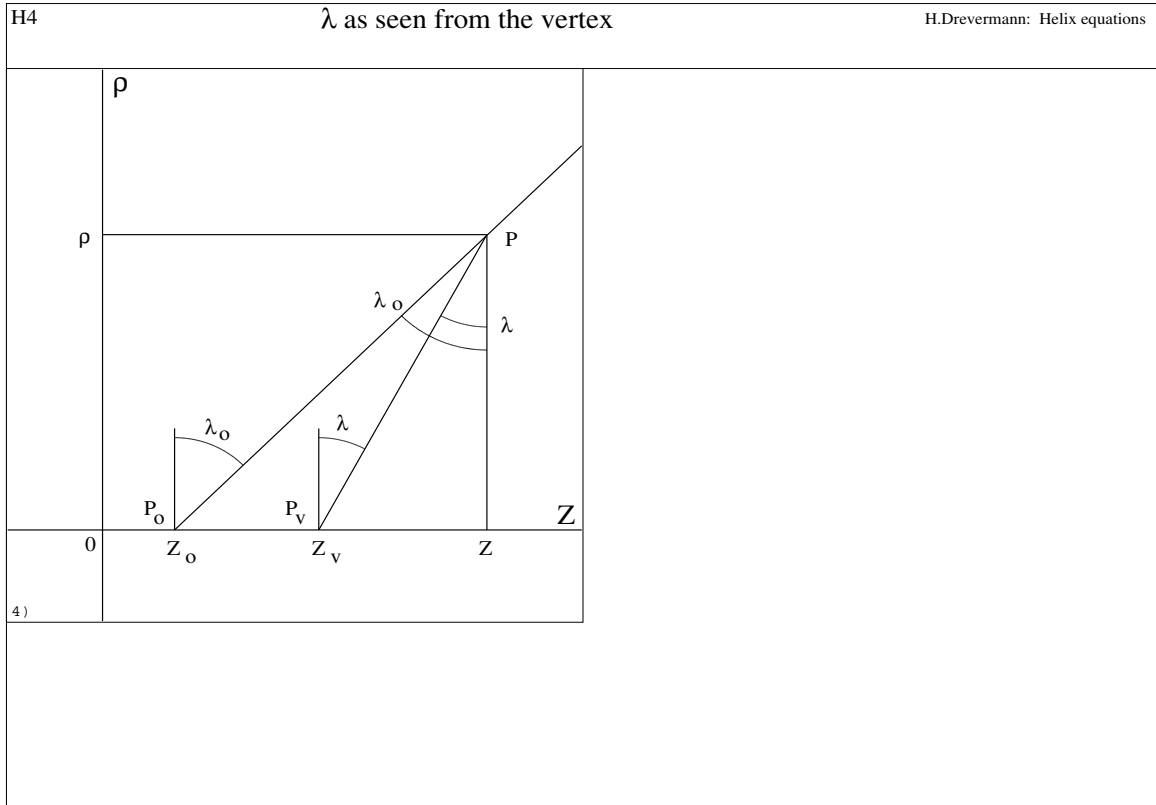


Figure 4: "λ as seen from the vertex"

The pdf file ed_bw_h4.pdf contains the figure in black and white.

The pdf file ed_co_h4.pdf contains the figure in color. When displaying the color picture the quality is better, if acroread is used.